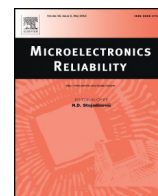




Contents lists available at ScienceDirect

## Microelectronics Reliability

journal homepage: [www.elsevier.com/locate/mr](http://www.elsevier.com/locate/mr)

## High temperature pulsed-gate robustness testing of SiC power MOSFETs

A. Fayyaz<sup>\*</sup>, A. Castellazzi

Power Electronics, Machines and Control Group, Department of Electrical and Electronic Engineering, University of Nottingham, University Park, Nottingham NG7 2RD, UK

## ARTICLE INFO

## Article history:

Received 2 June 2015

Received in revised form 21 June 2015

Accepted 30 June 2015

Available online xxx

## Keywords:

SiC

Power MOSFETs

Gate-oxide reliability

Robustness

Wide bandgap

SiC/SiO<sub>2</sub> interface

## ABSTRACT

Silicon Carbide (SiC) gate oxide reliability still remains a crucial issue and is amongst the important consideration factors when it comes to the implementation of SiC MOS-based devices within industrial power electronic applications. Recent studies have emerged assessing the gate oxide reliability of SiC MOSFETs. Such studies are needed in order to fully understand the properties of SiC/SiO<sub>2</sub> interface which is currently holding back the industry from fully utilising the superior features that SiC may offer. This paper aims to present experimental results showing the threshold voltage ( $V_{TH}$ ) and gate leakage current ( $I_{GSS}$ ) behaviour of SiC MOSFETs when subjected to pulsed-gate switching bias and drain-source bias stress at high temperature over time. The results obtained are then used to investigate the gate-oxide reliability of SiC MOSFETs. 2D TCAD static simulation results showing electric field distribution near the SiC/SiO<sub>2</sub> interface are also presented in this paper.

© 2015 Elsevier Ltd. All rights reserved.

## 1. Introduction

Silicon carbide (SiC), a wide bandgap (WBG) semiconductor material, is an attractive base material for making power transistors due to its better physical properties than silicon (Si) and has the potential to overcome the limitations imposed by power devices made of Si base material. A wider bandgap of around 3 eV, an about ten times higher critical electric field and an about three times higher thermal conductivity are some of the remarkable physical properties that SiC possess which are of particular relevance for power electronic applications [1].

The creation of metal oxide semiconductor (MOS) devices using SiC has been favoured compared to other WBG materials due to the presence of its stable native oxide (SiO<sub>2</sub>). As the oxide grows, carbon (C) atoms present in SiC crystal need to be removed by transport through the oxide in the form of CO or CO<sub>2</sub>. It has not been possible to fully remove the C atoms and hence unreacted carbon atoms result in formation of clusters which consequently lead to traps (defects) at the SiO<sub>2</sub>-SiC interface. Currently, the density of interface states ( $D_{it}$ ) at the SiC/SiO<sub>2</sub> interface is around  $10^{12} \text{ eV}^{-1} \text{ cm}^{-2}$  which is about two to three orders of magnitude higher than the comparatively matured Si/SiO<sub>2</sub> interface [2]. As discussed in [2,3], formation of Si dangling bonds, C dangling bonds and Oxygen (O) vacancies along with formation of C clusters are some of the widely used explanations in literature behind the cause of high  $D_{it}$ . Another drawback of having large  $D_{it}$  is the reduced interface mobility in the channel due to coulomb scattering phenomenon.

The critical electric field for SiC material is around ten times higher than the Si material and is also much higher than the SiO<sub>2</sub> [4]. Also, SiO<sub>2</sub> has a drawback that it has lower dielectric constant which is two and a half times lower than that of the SiC material [5]. Due to the above-mentioned reasons, SiC MOS devices are required to be operated at a lower electric field than the SiC critical electrical field in order to avoid the premature breakdown of SiO<sub>2</sub> at the device surface. However, the gate oxide can be shielded from the high electric field within the semiconductor with help of an enhanced MOSFET structure [4].

High temperature gate bias (HTGB) and high temperature reverse bias (HTRB) static tests are test standards widely used for reliability testing and semiconductor device qualification within the device manufacturing industry (see [6], for instance).

Recent advancements in the SiC MOS fabrication technology has resulted in an increased commercial availability of SiC MOSFETs with various different voltage and current ratings from various different manufacturers [7]. Therefore, an in-depth study of the gate oxide reliability is necessary before the SiC MOSFETs can be widely utilised within industrial power electronic applications.

The work proposed in this paper extends our previous work on HTGB and HTRB static tests on SiC MOSFETs which looked at the  $V_{TH}$  instability and  $I_{LEAK}$  evolution [8]. This work aims to present results showing the behaviour of threshold voltage ( $V_{TH}$ ) and gate leakage current ( $I_{GSS}$ ) of SiC MOSFETs when subjected to pulsed-gate switching bias and drain-source bias stress at high temperature over time during transient operation of these devices. The proposed test setup was designed in order to apply pulsed-gate bias and drain-source bias stress simultaneously at elevated temperature as opposed to doing them separately. By doing this, SiC MOSFETs, widely used in high switching frequency and high temperature applications, are subjected to stress in a much

<sup>\*</sup> Corresponding author.

E-mail address: [eexaf12@nottingham.ac.uk](mailto:eexaf12@nottingham.ac.uk) (A. Fayyaz).

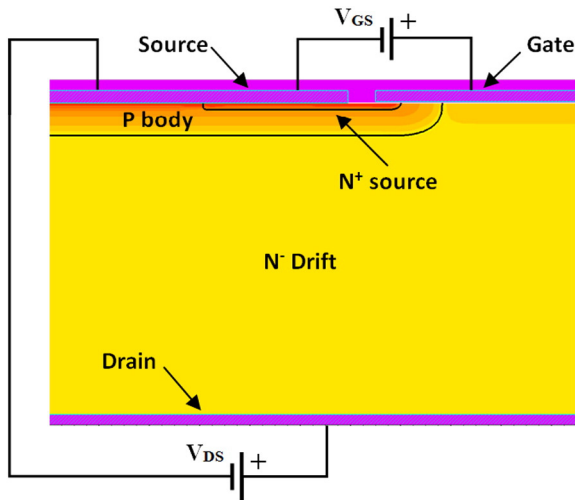


Fig. 1. SiC MOSFET half-cell planar structure.

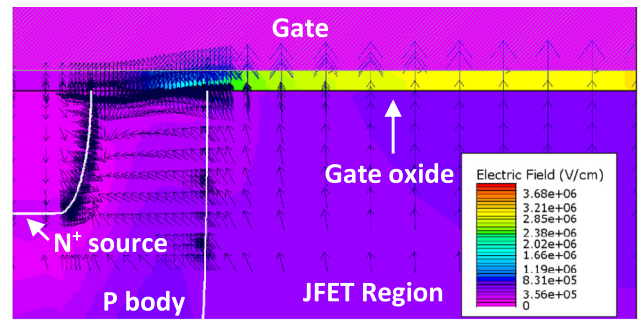
more realistic environment highly desired for power electronic industrial applications. 2D TCAD simulations showing electric field distribution near the SiC/SiO<sub>2</sub> interface are also included prior to the experimental results.

## 2. SiC MOSFET structure

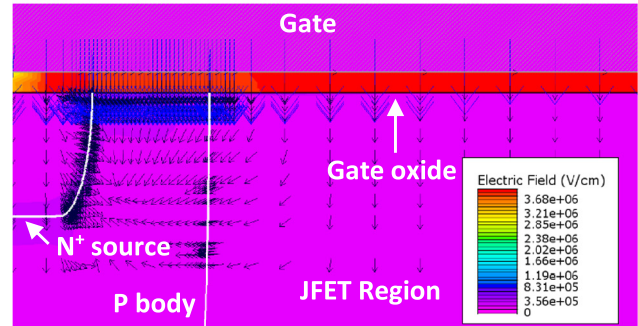
The half-cell structure of SiC Planar MOSFET is presented in Fig. 1. Static 2D TCAD physical simulations were carried out in order to show that the electric field ( $E$ ) distribution near the SiC–SiO<sub>2</sub> interface is much higher than in the drift region due to the difference in the dielectric constant of the oxide and the semiconductor as explained in the previous section. The simulations for electric field distributions near the SiC/SiO<sub>2</sub> interface for various test conditions are illustrated in Fig. 2. As mentioned earlier, the different dielectric constants in SiC and SiO<sub>2</sub> is one of the limitations to using SiC at its maximum field with-stand capability. Several studies have shown that the SiC devices can also be made with other dielectric materials to further enhance their performance [5,9].

The electric field distribution inside the gate oxide is very uniform for gate bias stress only as shown in Fig. 2b and c. The direction of the electric field would obviously be different depending on the polarity of the gate bias stress as shown. But on the other hand, for drain source bias ( $V_{DS} = 600$  V) in Fig. 2a, the electric field is maximum in the centre of the gate oxide and decreases towards the source as expected with decrease in the potential inside the JFET region.

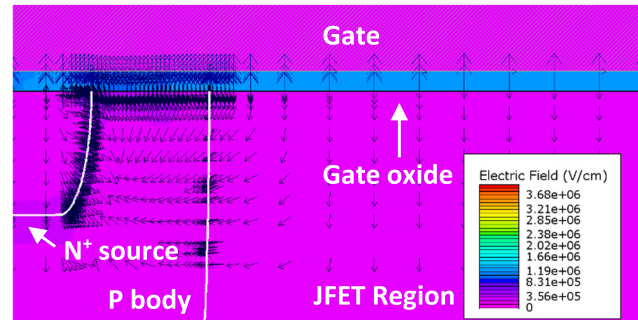
In Fig. 2d, the electric field in the gate oxide is maximum near the N<sup>+</sup> source for  $V_{DS} = 600$  V and  $V_{GS} = +20$  V and it decreases towards the centre of the gate oxide. On the other hand, for  $V_{DS} = 600$  V and  $V_{GS} = -5$  V, the electric field is the maximum in the middle of the gate oxide and it decreases towards the N<sup>+</sup> source as shown in Fig. 2e. It is worth noting that the maximum net electric field in the gate oxide is higher for negative gate bias with drain source bias (Fig. 2e) as compared to the case with just the negative gate stress and no  $V_{DS}$  (Fig. 2c). This is because for the earlier case, the direction of electric field produced due to  $V_{DS} = 600$  V and  $V_{GS} = -5$  V is positive from drain to gate and source to gate respectively. The opposite can be said for Fig. 2d since the direction of electric field due to  $V_{GS} = 20$  V and  $V_{DS} = 600$  V is positive from gate to source and positive from drain to



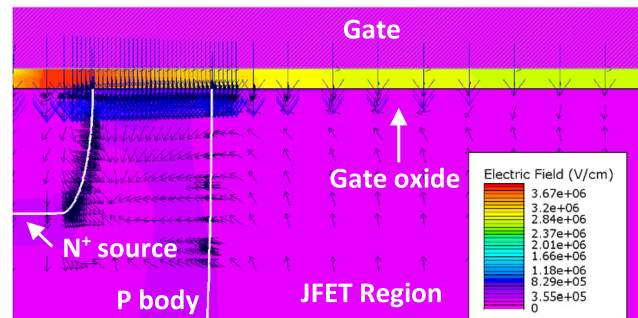
(a)  $V_{DS} = 600V$  and  $V_{GS} = 0V$



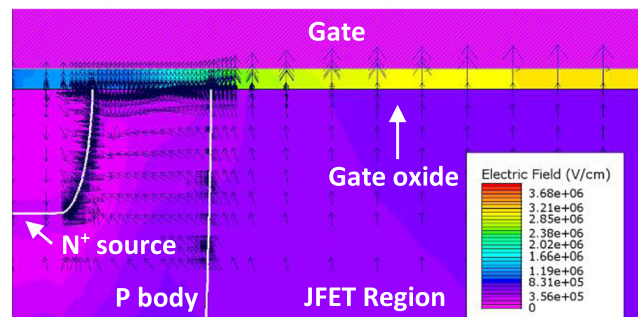
(b)  $V_{DS} = 0V$  and  $V_{GS} = 20V$



(c)  $V_{DS} = 0V$  and  $V_{GS} = -5V$



(d)  $V_{DS} = 600V$  and  $V_{GS} = 20V$



(e)  $V_{DS} = 600$  and  $V_{GS} = -5V$

Fig. 2. Simulation result showing electric field distribution near the SiC/SiO<sub>2</sub> interface at different bias conditions (Zoomed in). (a)  $V_{DS} = 600$  V and  $V_{GS} = 0$  V. (b)  $V_{DS} = 0$  V and  $V_{GS} = 20$  V. (c)  $V_{DS} = 0$  V and  $V_{GS} = -5$  V. (d)  $V_{DS} = 600$  V and  $V_{GS} = 20$  V. (e)  $V_{DS} = 600$  and  $V_{GS} = -5$  V.

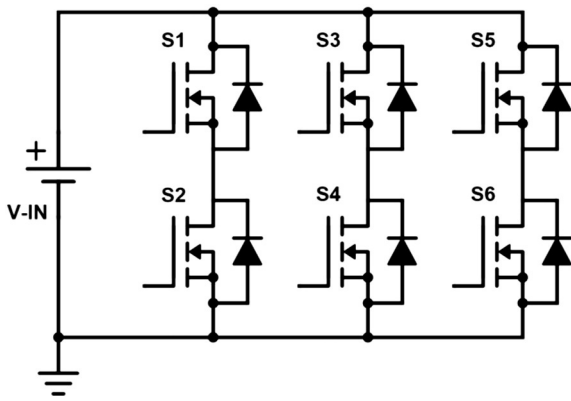


Fig. 3. Schematic of 3-phase Inverter test circuit with no load.

gate respectively. Therefore, the net electric field in the centre of gate oxide is smaller.

### 3. Experimental methodology and test setup

#### 3.1. Stress setup

The test circuit designed is a 2-level 3-phase inverter which is able to include six devices under test (DUTs) at a time. The DUTs are the latest generation commercially available 1200 V 36A rated TO-247 packaged SiC MOSFETs from CREE. The schematic of the implemented 3-phase inverter is shown in Fig. 3. The inverter operates without any load in order to be able to observe the change in  $V_{TH}$  and  $I_{GSS}$  induced purely due to pulsed-gate bias and drain-source bias stress without any current conduction through the DUTs. Current conduction is undesirable as it would not only lead to unnecessarily heat up of devices, but could also have an impact on the monitored parameters. Therefore, to understand the true effect that pulsed-gate bias and the high electric field due to drain-source bias stress has on the  $V_{TH}$  and  $I_{GSS}$ , DUTs did not conduct any current.

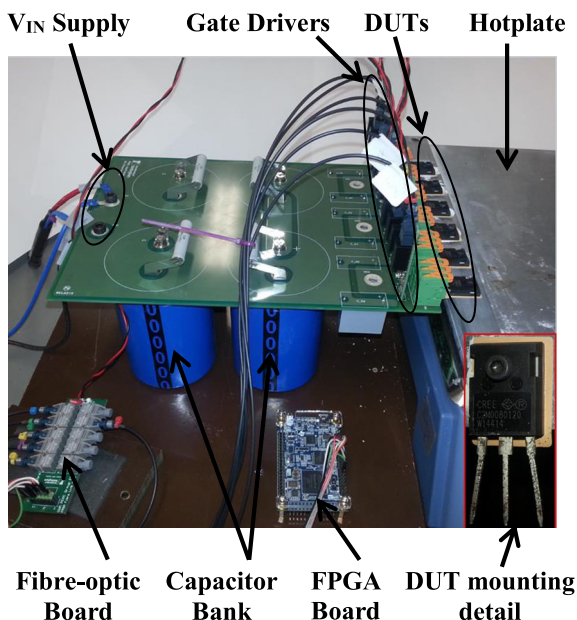


Fig. 4. 3-phase Inverter test circuit.

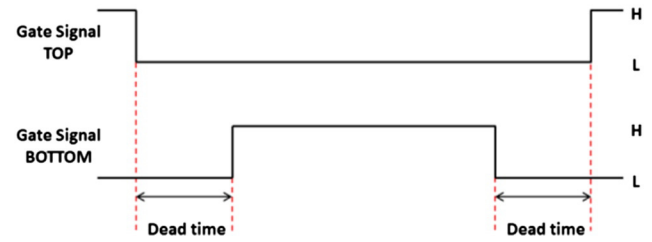
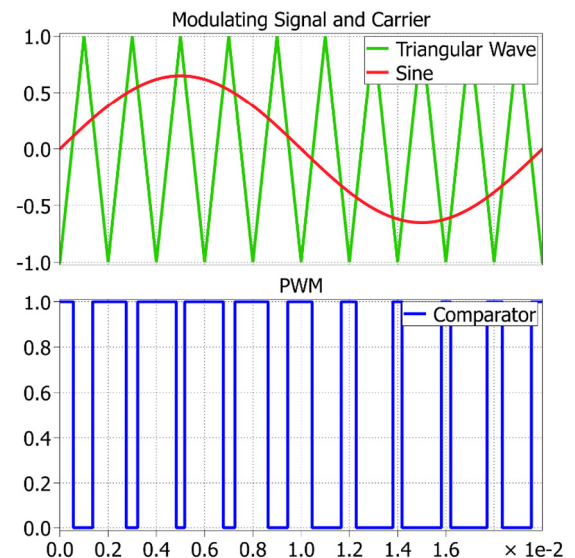


Fig. 5. Illustration of dead-time.

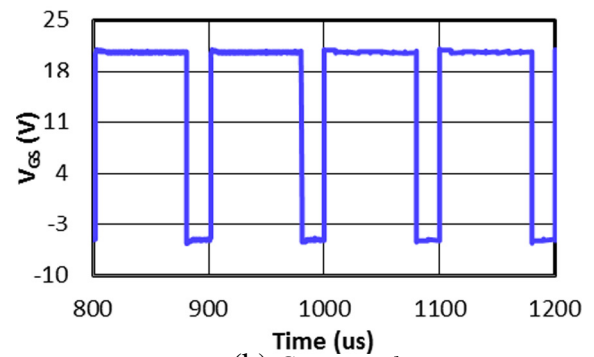
Fig. 4 shows the 3-phase inverter test circuit based on the circuit schematic in Fig. 3. A double sided 4 oz copper PCB board was used as a power plane and the gate drivers were vertically mounted onto the power PCB directly without wires in order to avoid voltage overshoot by minimising parasitic inductance. The devices are tightly screw mounted onto the hotplate as shown in the zoom-up (see inset) in Fig. 4.

The capacitor bank is rated at 900 V to allow ( $V_{IN}$ ) characterisation up to 900 V and the DUTs were mounted horizontally onto the hotplate to allow characterisation at different case temperatures ( $T_{CASE}$ ) up to 150 °C. This is a common setup that is also used for other tests and hence such big capacitors were used.

An open loop pulse width modulation (PWM) control was implemented to control the switching sequence of 6 DUTs using an Altera FPGA board. In an ordinary 3-phase inverter, the gate signal of the two switches in one leg should be complementary with an insertion of



(a) Illustration of PWM scheme



(b) Gate signal

Fig. 6. PWM scheme and resulting gate drive signal. (a) Illustration of PWM scheme. (b) Gate signal.



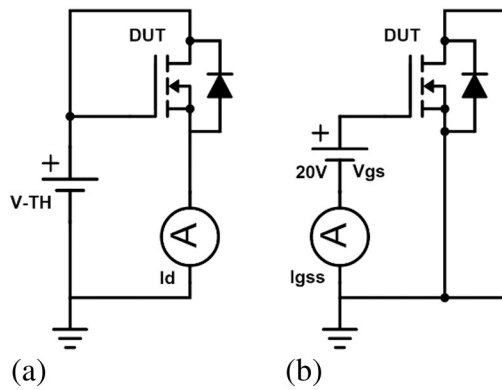


Fig. 7. Schematic for measuring (a)  $V_{TH}$  and (b)  $I_{GSS}$ .

dead-time between the commutations to avoid any shoot-through as illustrated in Fig. 5. The switching commutation in each leg is also phase-shifted by 120 °C but that is not really required here since there is no current conduction.

The switching frequency was 10 kHz (50 Hz sine modulating signal and 10 kHz triangular carrier signal) with a dead-time of 400 ns and a modulation index of 0.65. Dead-time of 400 ns was chosen since the devices are fast to turn ON and OFF with around 100 ns of rise and fall time respectively. Modulation index of 0.65 was chosen to represent industrial applications requiring 270 V sinusoidal rms output. The applied  $V_{GS}$  was switched between +20 V and –5 V. The illustration of PWM scheme and the gate signal is shown in Fig. 6a and b respectively. The carrier frequency in Fig. 6a (illustration purpose only) is much smaller than the actual carrier frequency in the experiment as it is very difficult to show the 10 kHz carrier signal for one period of the 50 Hz modulating signal.

When the top switch in a leg is ON and the bottom switch is OFF, the bottom switch blocks the full  $V_{IN}$  voltage. Once the top switch turns OFF, the bottom switch is still OFF due to the dead-time, the top and bottom switch will each have a blocking voltage of about  $V_{IN}/2$ . After the dead-time, the bottom switch will then turn ON and at this time, the top switch stays OFF therefore, the top switch will be blocking the full  $V_{IN}$  voltage. The  $V_{DS}$  of each device swing between 0 to  $V_{IN}/2$  and  $V_{IN}/2$  to  $V_{IN}$ .

### 3.2. Parameter monitoring setup

The circuit schematics for measuring  $V_{TH}$  and  $I_{GSS}$  are shown in Fig. 7a and b respectively. The  $V_{TH}$  was defined as the gate-source voltage at which the ammeter measuring drain current ( $I_D$ ) read 5 mA when  $V_{DS} = V_{GS}$ . The  $I_{GSS}$  was measured at  $V_{GS} = 20$  V. For measuring  $I_D$  and  $I_{GSS}$ , Keithley 6485 Picoammeter and 2635A System Sourcecrometer, capable of measuring dc current as small as 1 pA, were used respectively.

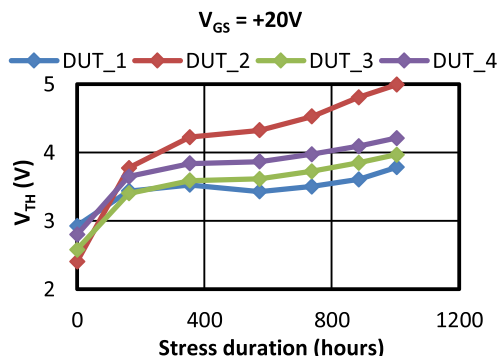


Fig. 8. High temperature gate-bias (HTGB) results.

Table 1  
Summary of test conditions for HTGB.

DUTs	$V_{GS}$ (V)	$V_{DS}$ (V)	$T_{CASE}$ (°C)	Duration (hours)
4	+20	0	150	1000

## 4. Experimental results and discussion

### 4.1. HTGB test

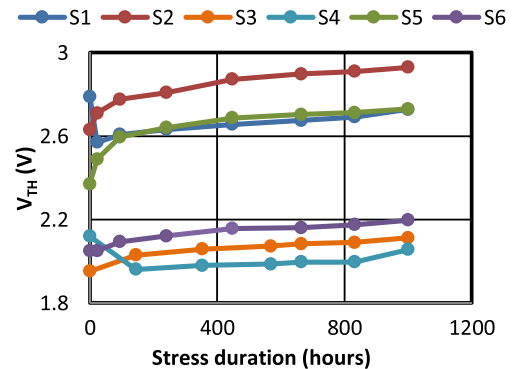
Some results for the HTGB static tests from our previous work (see [8] for more information) on SiC MOSFET reliability of the previous generation CREE devices are included here in Fig. 8. The summary of the test results is included in Table 1.

Results for positive gate-bias stress (Fig. 8) show that  $V_{TH}$  had a positive shift as the stress duration increased. The main point to be noted here is the huge  $V_{TH}$  instability when subjected to HTGB stress.

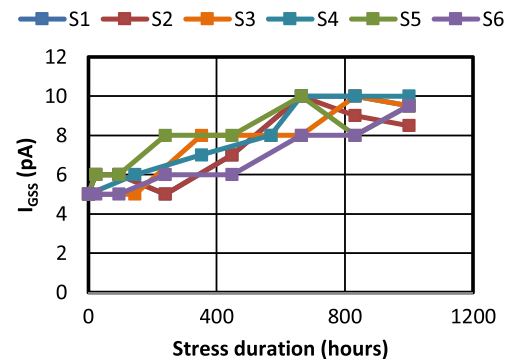
### 4.2. High temperature pulsed-gate switching testing

The devices were subjected to total stress duration of 1000 h of bias stress and the  $V_{TH}$  and  $I_{GSS}$  were measured at regular intervals. The behaviour of  $V_{TH}$  and  $I_{GSS}$  with respect to stress duration is plotted in Fig. 9a and b respectively for the test conditions mentioned in Table 2.

In Fig. 9a, it can be seen that  $V_{TH}$  mainly increases as the duration of stress increases. Initially, the change in  $V_{TH}$  is apparent but afterwards as the stress accumulates,  $V_{TH}$  seems quite stable with very small change in later values as compared to HTGB results where large  $V_{TH}$  instability was seen. The E distribution simulations clearly indicate that applying  $V_{DS}$  and positive  $V_{GS}$  bias in fact results in a smaller electric field in the



(a) Threshold voltage ( $V_{TH}$ ) evolution



(b) Gate leakage current ( $I_{GSS}$ ) evolution

Fig. 9. Evolution of monitored parameters;  $V_{IN} = 600$  V;  $V_{GS} = +20/-5$ ;  $T_{CASE} = 150$  °C. (a) Threshold voltage ( $V_{TH}$ ) evolution. (b) Gate leakage current ( $I_{GSS}$ ) evolution.

**Table 2**

Summary of test conditions for pulsed-gate switching test.

DUTs	$V_{GS}$ (V)	$V_{IN}$ (V)	$T_{CASE}$ (°C)	Duration (hours)
6	+20/−5	600	150	1000

oxide than for the case of positive  $V_{GS}$  bias alone (see Fig. 2b and d). Whereas on the other hand, the simulations clearly indicate that applying  $V_{DS}$  and negative  $V_{GS}$  bias in fact results in a higher electric field in the oxide than for the case of negative  $V_{GS}$  bias alone (see Fig. 2c and e).

When positive gate source voltage ( $V_{GS}$ ) bias is applied to turn ON the device by forming a channel, the electrons get attracted to the positive gate potential i.e. the SiC/SiO<sub>2</sub> interface where a small concentration will get injected into the oxide. As mentioned earlier, the SiC/SiO<sub>2</sub> interface contains traps which are created during the oxidation process. When the electrons move through the oxide layer due to the electric field produced due to  $V_{GS}$  and  $V_{DS}$ , a proportion of them get trapped in the interface traps which then leads to negatively charged centres. In order to overcome the additional negative charge due to the trapped negative charge, a larger potential difference i.e.  $V_{TH}$  will be required to turn ON the device [7]. The results in Fig. 9a (also in Fig. 8) clearly demonstrate that this physical phenomenon is taking place inside the devices. And the opposite can be said for the negative gate-bias stress since the electrons move out of the traps and hence a lower  $V_{TH}$  potential would be required to turn ON the device. Moreover, another reason of the net positive shift in  $V_{TH}$  seen for pulsed-gate bias stress could be due to the modulation index of 0.65 which meant the devices were ON (positive bias at +20 V) for 65% and OFF (negative bias at −5 V) for 35% of the total stress duration. It would also be interesting to see the  $V_{TH}$  evolution if the modulation index is less than 0.5.

Fig. 9b shows the  $I_{GSS}$  behaviour when subjected to the pulsed-gate stress. It increases slightly in the beginning but towards the end of the stress duration, it seems quite stable. However, no big changes in the  $I_{GSS}$  were observed. Due to the nature of the measurement ( $I_{GSS}$ ), an average value was taken since the measurement is too small and is prone to sensitivity hence the readings fluctuated a lot. Every possible effort was made to have as accurate measurement as possible for  $I_{GSS}$ .

## 5. Conclusion

Pulsed-gate switching bias tests were performed on the latest generation CREE SiC MOSFETs in order to characterise its gate oxide reliability. In order to do that, DUTs were subjected to pulsed-gate bias and drain-source bias stress. The parameters named  $V_{TH}$  and  $I_{GSS}$  were monitored at regular intervals and the changes in these parameters were recorded. The test setup was designed to subject the DUTs to more realistic power electronic operating conditions. The results have shown that the change in  $V_{TH}$  for pulsed-gate bias stress is much smaller than for HTGB with positive bias. The reason for this is clearly the smaller electric field due to  $V_{DS}$  bias as shown in simulations.

## References

- [1] M. Treu, R. Rupp, G. Sölkner, Reliability of SiC power devices and its influence on their commercialization — review, status, and remaining issues, IEEE IRPS 2010, pp. 156–161.
- [2] P.A. Mawby, C. Kampouris, A. Koh, Advances in silicon carbide MOS technology, Proc. 23rd International Conference on Microelectronics, vol. 1, May 12–15 2002 (Nis, Yugoslavia).
- [3] E. Pippel, J. Woltersdorf, H.Ö. Ölafsson, E.Ö. Sveinbjörnsson, Interfaces between 4H-SiC and SiO<sub>2</sub>: microstructure, nanochemistry, and near-interface traps, J. Appl. Phys. 97 (3) (2005) 034302.
- [4] T.T. Nguyen, A. Ahmed, T.V. Thang, J.H. Park, Gate oxide reliability issues of SiC MOSFETs under short-circuit operation, IEEE Trans. Power Electron. 30 (5) (2015) 2445–2455 (Chicago).
- [5] M. Nawaz, On the evaluation of gate dielectrics for 4H-SiC based power MOSFETs, Act. Passive Electron. Compon. 2015 (December 2014) 1–12.
- [6] R. Green, A. Lelis, D. habersat, Application of reliability test standards to SiC power MOSFETs, Reliability Physics Symposium (IRPS). IEEE International 2011, pp. ex.2.1–ex.2.9.
- [7] Mrinal K. Das, et al., SiC MOSFET reliability update, Mater. Sci. Forum 717 (2012).
- [8] L. Yang, A. Castellazzi, High temperature gate-bias and reverse-bias tests on SiC MOSFETs, Microelectron. Reliab. 53 (9–11) (September–November 2013) 1771–1773.
- [9] J. Robertson, High dielectric constant oxides, Eur. Phys. J. Appl. Phys. (March 2004) 265–291.